



**HAL**  
open science

## Intermediate mass dimuons in NA38/NA50

M C. Abreu, B. Alessandro, C. Alexa, R. Arnaldi, J. Astruc, M. Atayan, C. Baglin, A. Baldit, M. Bedjidian, F. Bellaiche, et al.

► **To cite this version:**

M C. Abreu, B. Alessandro, C. Alexa, R. Arnaldi, J. Astruc, et al.. Intermediate mass dimuons in NA38/NA50. International Conference on Strangeness in Quark Matter 4, Jul 1998, Padova, Italy. pp.235-245. in2p3-00002426

**HAL Id: in2p3-00002426**

**<https://hal.in2p3.fr/in2p3-00002426>**

Submitted on 28 Apr 1999

**HAL** is a multi-disciplinary open access archive for the deposit and dissemination of scientific research documents, whether they are published or not. The documents may come from teaching and research institutions in France or abroad, or from public or private research centers.

L'archive ouverte pluridisciplinaire **HAL**, est destinée au dépôt et à la diffusion de documents scientifiques de niveau recherche, publiés ou non, émanant des établissements d'enseignement et de recherche français ou étrangers, des laboratoires publics ou privés.

## Intermediate mass dimuons in NA38/NA50<sup>1</sup>

E. Scomparin<sup>5,g)</sup> – *NA50 collaboration*

M.C. Abreu<sup>6,a)</sup>, B. Alessandro<sup>11)</sup>, C. Alexa<sup>3)</sup>, R. Arnaldi<sup>11)</sup>, J. Astruc<sup>8)</sup>,  
M. Atayan<sup>13)</sup>, C. Baglin<sup>1)</sup>, A. Baldit<sup>2)</sup>, M. Bedjidian<sup>12)</sup>, F. Bellaiche<sup>12)</sup>, S. Beolè<sup>11)</sup>,  
V. Boldea<sup>3)</sup>, P. Bordalo<sup>6,b)</sup>, A. Bussière<sup>1)</sup>, V. Capony<sup>1)</sup>, L. Casagrande<sup>6)</sup>,  
J. Castor<sup>2)</sup>, T. Chambon<sup>2)</sup>, B. Chaurand<sup>9)</sup>, I. Chevrot<sup>2)</sup>, B. Cheynis<sup>12)</sup>,  
E. Chiavassa<sup>11)</sup>, C. Cicalò<sup>4)</sup>, M.P. Comets<sup>8)</sup>, S. Constantinescu<sup>3)</sup>, J. Cruz<sup>6)</sup>, A. De  
Falco<sup>4)</sup>, N. De Marco<sup>11)</sup>, G. Dellacasa<sup>11,c)</sup>, A. Devaux<sup>2)</sup>, S. Dita<sup>3)</sup>, O. Drapier<sup>12)</sup>,  
B. Espagnon<sup>2)</sup>, J. Fargeix<sup>2)</sup>, S.N. Filippov<sup>7)</sup>, F. Fleuret<sup>9)</sup>, P. Force<sup>2)</sup>, M. Gallio<sup>11)</sup>,  
Y.K. Gavrillov<sup>7)</sup>, C. Gerschel<sup>8)</sup>, P. Giubellino<sup>11)</sup>, M.B. Golubeva<sup>7)</sup>, M. Gonin<sup>9)</sup>,  
A.A. Grigorian<sup>13)</sup>, J.Y. Grossiord<sup>12)</sup>, F.F. Guber<sup>7)</sup>, A. Guichard<sup>12)</sup>, H. Gulkanyan<sup>13)</sup>,  
R. Hakobyan<sup>13)</sup>, R. Haroutunian<sup>12)</sup>, M. Idzik<sup>11,d)</sup>, D. Jouan<sup>8)</sup>, T.L. Karavitcheva<sup>7)</sup>,  
L. Kluberg<sup>9)</sup>, A.B. Kurepin<sup>7)</sup>, Y. Le Bornec<sup>8)</sup>, C. Lourenço<sup>5)</sup>, M. Mac Cormick<sup>8)</sup>,  
P. Macciotta<sup>4)</sup>, A. Marzari-Chiesa<sup>11)</sup>, M. Maserà<sup>11)</sup>, A. Masoni<sup>4)</sup>, S. Mehrabyan<sup>13)</sup>,  
S. Mourgues<sup>2)</sup>, A. Musso<sup>11)</sup>, F. Ohlsson-Malek<sup>12,e)</sup>, P. Petiau<sup>9)</sup>, A. Piccotti<sup>11)</sup>,  
J.R. Pizzi<sup>12)</sup>, W.L. Prado da Silva<sup>11,f)</sup>, G. Puddu<sup>4)</sup>, C. Quintans<sup>6)</sup>, C. Racca<sup>10)</sup>,  
L. Ramello<sup>11,c)</sup>, S. Ramos<sup>6,b)</sup>, P. Rato-Mendes<sup>11)</sup>, L. Riccati<sup>11)</sup>, A. Romana<sup>9)</sup>,  
S. Sartori<sup>11)</sup>, P. Saturnini<sup>2)</sup>, E. Scomparin<sup>5,g)</sup>, S. Serçi<sup>4)</sup>, R. Shahoyan<sup>6,h)</sup>, S. Silva<sup>6)</sup>,  
C. Soave<sup>11)</sup>, P. Sonderegger<sup>5,b)</sup>, X. Tarrago<sup>8)</sup>, P. Temnikov<sup>4)</sup>, N.S. Topilskaya<sup>7)</sup>,  
G.L. Usai<sup>4)</sup>, C. Vale<sup>6)</sup>, E. Vercellin<sup>11)</sup>, N. Willis<sup>8)</sup>.

*Accepted by Journal of Physics G*

---

<sup>1</sup>Talk given at the 4<sup>th</sup> International Conference on Strangeness in Quark Matter – Padova, July 20–24, 1998.

## Abstract

The NA38/NA50 experiments have measured, at the CERN SPS, the dimuon production in proton–nucleus and nucleus–nucleus collisions. In this paper it is shown that the mass continuum between the  $\phi$  and the  $J/\psi$  can be satisfactorily described, after having removed the combinatorial background due to uncorrelated  $\pi$  and  $K$  decays, as a sum of two contributions, namely the Drell–Yan process and the semi–leptonic decay of pairs of charmed mesons, whose mass shape in the acceptance of the experiment has been evaluated using PYTHIA. However, in order to describe the A–B (namely S–U and Pb–Pb) mass spectra, the dimuon yield from open charm decays, which in p–A collisions is found to be consistent with direct open charm measurements from other CERN and FNAL experiments, has to be enhanced with respect to a linear extrapolation of p–A results. The size of the enhancement smoothly increases from peripheral S–U to central Pb–Pb interactions, reaching a factor  $\sim 3$  in central Pb–Pb collisions. The  $p_T$  distributions of the events in the mass continuum are also compatible with the hypothesis of open charm enhancement in A–B collisions.

- 
- 1) LAPP, CNRS-IN2P3, Annecy-le-Vieux, France.
  - 2) LPC, Univ. Blaise Pascal and CNRS-IN2P3, Aubière, France.
  - 3) IFA, Bucharest, Romania.
  - 4) Università di Cagliari/INFN, Cagliari, Italy.
  - 5) CERN, Geneva, Switzerland.
  - 6) LIP, Lisbon, Portugal.
  - 7) INR, Moscow, Russia.
  - 8) IPN, Univ. de Paris-Sud and CNRS-IN2P3, Orsay, France.
  - 9) LPNHE, Ecole Polytechnique and CNRS-IN2P3, Palaiseau, France.
  - 10) IReS, Univ. Louis Pasteur and CNRS-IN2P3, Strasbourg, France.
  - 11) Università di Torino/INFN, Torino, Italy.
  - 12) IPN, Univ. Claude Bernard and CNRS-IN2P3, Villeurbanne, France.
  - 13) YerPhI, Yerevan, Armenia.
- a) also at FCUL, Universidade de Lisboa, Lisbon, Portugal
  - b) also at IST, Universidade Técnica de Lisboa, Lisbon, Portugal
  - c) Dipartimento di Scienze e Tecnologie Avanzate, II Facoltà di Scienze, Alessandria, Italy
  - d) now at Faculty of Physics and Nuclear Techniques, University of Mining and Metallurgy, Cracow, Poland
  - e) now at ISN, Univ. Joseph Fourier and CNRS-IN2P3, Grenoble, France
  - f) now at UERJ, Rio de Janeiro, Brazil
  - g) on leave of absence from Università di Torino/INFN, Torino, Italy
  - h) on leave of absence of YerPhI, Yerevan, Armenia

# 1 Introduction

The study of the dilepton yield has always been, from the conceptual point of view, one of the most promising topics in the field of ultra-relativistic heavy-ion collisions; the absence of strong interactions with the surrounding hadronic medium allows them to carry out information about the conditions of the nuclear matter at early times in the history of the collision, and possibly revealing the formation of a hot QGP phase [1].

The experimental study of dilepton production, however, is far from being trivial, since dileptons from different sources are often superimposed in the phase space, and it can be difficult to disentangle the various contributions in an unambiguous way.

The study of the vector mesons  $\rho$ ,  $\omega$ ,  $\phi$ ,  $J/\psi$  via their leptonic decay is less affected by these problems, since they appear as more or less pronounced structures in the dilepton invariant mass spectra.

On the contrary, the analysis of the mass continua between the threshold and the  $\rho$  (the so called low-mass region, or LMR), and between the  $\phi$  and the  $J/\psi$  (the so called intermediate-mass region, or IMR), is made difficult by the overlap of several sources with non-resonant patterns (Dalitz decays of light mesons, semileptonic decays of charmed meson pairs, Drell-Yan process), and by the presence of a large combinatorial background ( $\pi$  and  $K$  uncorrelated decays).

In this paper we present an analysis of the IMR dimuon spectrum, measured in p-A (A=Al, Cu, Ag, W) collisions at 450 GeV incident energy, in S-U at 200 GeV/nucleon and in Pb-Pb at 158 GeV/nucleon, by the NA38 and NA50 experiments at the CERN SPS. The study of this mass region is particularly interesting since thermal dimuons from the 'hot' phase could produce a detectable signal in the IMR, where the hadronic resonance contributions are negligible, and the contributions from hard processes (Drell-Yan, open charm) can be calculated.

Early NA38/NA50 studies [2, 3] showed that the A-B dimuon yield in the IMR for nucleus-nucleus collisions could not be described as a linear extrapolation of the p-A results; the presence of an 'excess' was established but, mainly because of the low statistics and of the limits of the adopted background subtraction techniques, it was not possible to speculate on its origin. A similar result has also been obtained by the HELIOS-3 collaboration [4], comparing the dimuon production in S-W and p-W interactions over a large kinematical region.

In the present analysis a slightly different approach has been chosen; namely, where an excess is known to be present (i.e. in nucleus-nucleus collisions) its description has been attempted, both in the mass and transverse momentum variables, by means of an enhancement of the sources already present in p-nucleus collisions, without referring to any new contributions, as thermal dimuons.

## 2 Apparatus and data reduction

The NA38 experiment consisted mainly of a muon spectrometer [5]; the tracks were deflected by a toroidal magnet, and reconstructed using two sets of four MWPCs. Muon pairs were detected in the pseudorapidity interval  $2.8 < \eta < 4.0$ . NA50 is the upgraded version of the experiment for the study of Pb–Pb interactions at 158 GeV/nucleon. The NA50 apparatus was also used for the study of the p–A systems considered in this analysis.

Detailed descriptions of the various set-ups can be found elsewhere [6, 7], and only the main features will be recalled hereafter.

### 2.1 NA38 set-up (S–U collisions)

The NA38 data used in this paper were taken with the spectrometer operated with a toroidal magnetic field of 1.2 Tm, and separated from the target region by a 4 m long hadron absorber made of carbon, followed by 0.8 m of iron. A segmented active target, made of 12 U subtargets, corresponding to a thickness of  $0.2\lambda_i$ , provided the identification of the primary vertex. The centrality of the collision was measured through an electromagnetic calorimeter (EMcal), positioned in front of the hadron absorber, and covering the pseudorapidity interval  $1.7 < \eta < 4.1$ . The apparatus included also a beam hodoscope of scintillation counters to tag the incident ion and to reject pile-up. The beam intensity was about  $10^8$  S ions/burst, with a 5 s spill.

### 2.2 NA50 set-up (Pb–Pb, p–A collisions)

In NA50, because of the much higher radiation level and hadron multiplicities induced by the Pb beam, an upgrade of the apparatus was necessary. Firstly, the field in the spectrometer has been raised to 2.1 Tm, in order to reduce the rate of soft background muons and improve the resolution in the  $J/\psi$  mass region. The data analyzed in this paper have been collected with an active target [8] made of 7 Pb subtargets, with a total thickness of  $0.3\lambda_i$ . The pseudorapidity coverage of the EMcal has been shifted to  $1.1 < \eta < 2.3$ ; furthermore, a zero-degree calorimeter (ZDC) [9] and a multiplicity detector (MD) have been introduced, to get a more complete characterization of the collision geometry. Beam hodoscopes and active target detectors have been re-built using quartz instead of plastic scintillators. With such a set-up the experiment has run at a beam intensity of  $5 \cdot 10^7$  Pb ions/burst, with a 5 s spill.

A similar set-up has been used for the p–A runs. Four nuclear targets have been used, namely Al, Cu, Ag and W. The active target system has been replaced by single targets with thicknesses ranging from  $32 \text{ g/cm}^2$  (Al) to  $80 \text{ g/cm}^2$  (W), with no vertex identification. No beam hodoscope has been used. The beam intensity was about  $3 \cdot 10^9$  protons/burst, with a 2.5 s spill.

## 2.3 Data reduction

The event selection criteria are quite similar for the various systems considered in this analysis. For both p–nucleus and nucleus–nucleus samples, the selected events must have two and only two fully reconstructed tracks in the muon spectrometer; furthermore, the two tracks must point to the target. These quality cuts are very effective since they reject more than 50% of the triggered events.

For S–U and Pb–Pb samples, the beam hodoscope information is used to reject events with more than one incident ion in a 20 ns gate opened by the trigger. In p–A runs, the undetected pile–up of beam particles can produce fake dimuons; this non–negligible contribution, due to the high beam intensity, adds to the combinatorial background and particular care has to be taken in its subtraction.

For S–U the information from the target detectors is used to select events with only one interaction. The identification of the interaction subtarget has a low efficiency for peripheral collisions. In Pb–Pb, where the ZDC information is available, a less restrictive selection can be adopted; since events coming from the target region must be strongly correlated in the  $E_T$  vs  $E_{ZDC}$  plane, only the events lying in a  $2\sigma$  region around the average correlation are retained.

Finally, in order to reject dimuons coming from kinematical regions where the acceptance is very low, only events with  $-0.5 < \cos\theta_{CS} < 0.5$ , where  $\theta_{CS}$  is the polar angle of the muons relative to the beam axis in the rest frame of the dimuon, have been accepted. For the same reason, the cut  $0 < y_{cm} < 1$  has been applied to dimuons from S–U and Pb–Pb collisions. For p–A interactions, due to the different incident energy, which leads to a different  $y_{cm}$  coverage, events with  $-0.52 < y_{cm} < 0.48$  have been selected.

## 2.4 Centrality selection

In the analysis of the nucleus–nucleus data the neutral transverse energy,  $E_T$ , measured event by event in the EMcal, has been used to group S–U and Pb–Pb data respectively in 5 and 9 centrality classes. The average number of participants and impact parameter for each centrality class have been estimated by means of a geometrical model [10], taking into account realistic nuclear densities. The results were further checked using a simulation based on the VENUS 4.02 [11] event generator.

## 3 Combinatorial background

In nucleus–nucleus collisions, because of the high hadron multiplicity, an important  $\mu^+\mu^-$  source is the in–flight decay of pairs of  $\pi$  and  $K$  mesons; of course, the same mechanism produces  $\mu^+\mu^+$  and  $\mu^-\mu^-$  pairs. The formula

$$N_{Bg}^{+-} = 2R\sqrt{N^{++}N^{--}} \quad (1)$$

with  $R=1$  can be used to estimate the number  $N_{Bg}^{+-}$  of background dimuons in the  $\mu^+\mu^-$  sample, from the measured number of like-sign events ( $N^{++}$ ,  $N^{--}$ ), if the trigger and the acceptance treat in the same way the different charge combinations and if the kinematical distributions of the parent ( $\pi$  and  $K$ ) mesons are not charge correlated. The same formula can be used for differential quantities, i.e. to calculate  $dN_{Bg}^{+-}/dM$ , or  $dN_{Bg}^{+-}/dp_T$ . The first requested condition for having  $R=1$  (no trigger/acceptance bias) is met in this analysis, thanks to the event selection introduced at the data reduction level; the charge uncorrelation hypothesis, which is valid for very high multiplicity events, is not fulfilled in p-A interactions, or in very peripheral nucleus-nucleus collisions, where  $R > 1$  is expected.

The choice of the  $R$ -factor is very important to this study, since in the IMR the contribution of the combinatorial background is rather high. Assuming  $R=1$ , as a first guess, in central Pb-Pb collisions 90% of the total IMR opposite sign dimuons comes from this source; even in p-A, because of the considerable pile-up levels connected with the high beam intensity, the percentage of background amounts to more than 80%.

Since an accurate determination of  $R$  is crucial, a detailed Monte-Carlo evaluation of this quantity has been carried out. For each of the various p-A and A-B systems analyzed,  $10^5$  events have been generated using VENUS; for each event the  $\pi$  and  $K$  four-momenta have been stored, the mesons have been tracked through the apparatus and the corresponding decay probabilities into muons  $P_{\mu_i}$ , with  $i = 1, N_\pi + N_K$ , have been calculated. Then, event by event, all the possible muon decay pairs falling in the spectrometer's acceptance have been considered, assigning to the produced dimuons the product of the single muon weights,  $P_{\mu\mu_{i,j}} = P_{\mu_i}P_{\mu_j}$ . Finally  $R^{MC}$  has been calculated from the sample of  $N$  events as

$$R^{MC} = \frac{\sum_{n=1}^N \sum_{i,j} P_{\mu\mu_{i,j}}^{+-}}{2\sqrt{(\sum_{n=1}^N \sum_{i,j} P_{\mu\mu_{i,j}}^{++})(\sum_{n=1}^N \sum_{i,j} P_{\mu\mu_{i,j}}^{--})}} \quad (2)$$

For Pb-Pb and S-U collisions, where  $R$  is expected to depend on the centrality, several calculations have been carried out at fixed impact parameter values, and the correlation between  $R^{MC}$  and  $b$  has been derived. Then, for each centrality class used in the analysis, the average value  $\langle R \rangle$  has been obtained as a weighted average of  $R^{MC}(b)$  over the  $b$  distribution of the events in that class. As a result, for the most central Pb-Pb collisions,  $\langle R \rangle$  is found to be compatible with 1, while for the peripheral bins  $\langle R \rangle$  becomes larger than 1; for the most peripheral bin, corresponding to  $\langle b \rangle = 10.7$  fm, the calculation gives  $\langle R \rangle = 1.035$ .

For p-A collisions the simulation must take into account that, because of the high beam intensity,  $\pi$  and  $K$  produced in several interactions (on the average 6 in p-W) are piled-up and seen as a single event by the detector. This effect smears the charge correlation between the parent mesons and leads to  $R^{MC}$  values close to 1. As an example, for p-W collisions,  $R^{MC}$  changes from 1.21, for a low beam intensity, to  $R^{MC} = 1.05$ , for the beam intensity used in the experiment.

In Pb–Pb collisions, where  $N_{BCK}^{+-}/N^{+-} \sim 0.9$ , the mass and  $p_T$  shapes of the combinatorial background must be known to a high degree of accuracy, to keep the error on the background-subtracted spectra at a reasonable level; therefore they have been calculated, for each centrality bin, with a method based on the combinations of muons from different like–sign events [12], and then normalized to  $2\langle R \rangle \sqrt{N^{++}N^{--}}$ .

## 4 The analysis

### 4.1 Introduction

The IMR is defined as the region of the mass spectrum between the  $\phi$  and the  $J/\psi$  where, after background subtraction, the known dimuon sources are the Drell–Yan process ( $DY$ ) and the semi–leptonic decays of charmed hadron pairs ( $D\bar{D}$ ). A reasonable lower limit for the IMR is  $M_{\mu\mu}=1.5$  GeV/ $c^2$ , where the contribution from the tails of the low–mass hadronic resonances is certainly negligible. As an upper limit,  $M_{\mu\mu}=2.5$  GeV/ $c^2$  is a suitable choice, since at higher masses the  $J/\psi$  starts to play a role, because of the finite resolution of the apparatus.

The analysis of the IMR described in this paper proceeds in various steps. First we calculate the shapes of the dimuon invariant mass distributions generated by the two processes ( $DY$ ,  $D\bar{D}$ ), in the acceptance of the experiment; then, the measured IMR distributions are described as a superposition of these two shapes, taking into account the constraints that help fixing their normalizations.

The absolute normalization for the dimuon component from  $DY$  can be constrained by the mass region above the  $J/\psi$  (high mass region, HMR), where  $DY$  is the only dimuon source at SPS energies. The normalization of the calculated  $DY$  mass shape can be easily adjusted to reproduce the data in that region, fixing in this way the  $DY$  contribution in the IMR. Furthermore, the high–mass  $DY$  dimuons have been the object of extensive studies by NA38/NA50; their production cross section, after correcting for isospin effects, is known and has been found to scale with  $A$  in p–A collisions, and with  $A \cdot B$  in A–B collisions [13].

The normalization of the  $D\bar{D}$  contribution is obtained by fitting the measured IMR mass spectra. The resulting values are then compared to the expected numbers, based on the direct measurements of CERN and FNAL experiments.

### 4.2 $DY$ and $D\bar{D}$ mass shapes

The mass distributions from  $DY$  and  $D\bar{D}$  decays, in the spectrometer acceptance, have been generated using PYTHIA [14], with the MRS A set of PDFs [15], and with  $m_c=1.5$  GeV/ $c^2$  and  $\langle k_T^2 \rangle=0.8$  GeV $^2$ . The generation has been done on a kinematical region larger than the one covered by the experiment, to take into account smearing effects, basically due to multiple scattering and energy loss in the hadron absorber. The muons have been tracked through the experimental set–up and, for the accepted



events, their kinematical variables have been reconstructed using the procedure applied to experimental data. Figure 1 shows the generated and reconstructed mass spectra for the two processes, for the Pb–Pb set–up.

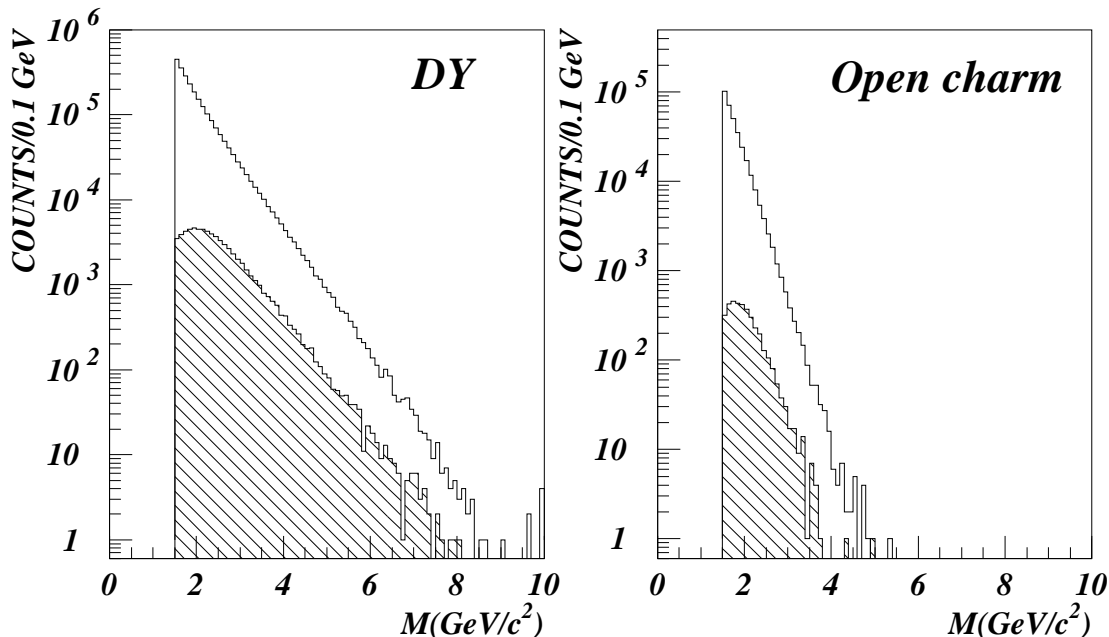


Figure 1: Generated (plain histogram) and reconstructed (filled histogram)  $DY$  and open charm dimuon invariant mass spectra.

The detector’s acceptance in a certain phase space region, for each process, is calculated by the ratio between the number of reconstructed and generated events in that region. For Pb–Pb, the acceptances for  $DY$  and  $D\bar{D}$ , for  $M > 1.5$   $\text{GeV}/c^2$  and in the  $\Delta y$  and  $\Delta \cos\theta$  domains defined above, are  $A_{DY} = 2.8\%$  and  $A_{D\bar{D}} = 1.1\%$ . Similar values have been obtained for the p–A data sets, since the experimental set–ups are practically identical. For S–U collisions, because of the lower value of the field in the toroidal magnet, the acceptances in the same phase space domain were higher by about a factor 4.

### 4.3 The fit of the mass spectra

The p–A data sets considered in this analysis have been taken using four nuclear targets (Al, Cu, Ag, W) at 450 GeV incident energy, always with the same experimental set–up.

To describe the mass spectra, a fit, in the mass range  $1.5 < M < 8.0$   $\text{GeV}/c^2$ , has been performed, keeping as free parameters the normalizations of the dimuon sources.

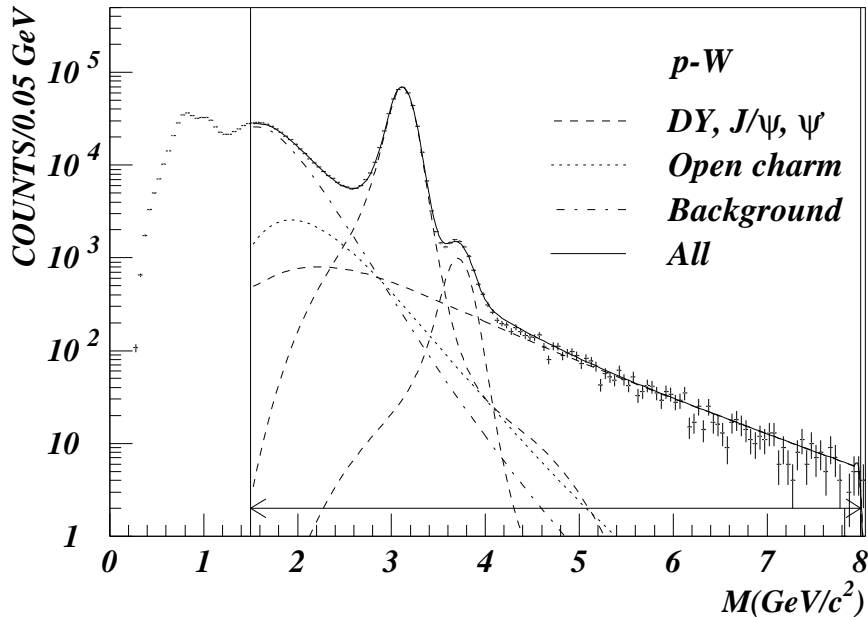


Figure 2: Fit to the p–W invariant mass spectrum, with the background fixed. The arrows indicate the region where the fit is performed.

In this mass region the contribution of the  $J/\psi$  and  $\psi'$  resonances must be taken into account; therefore their mass shapes have been calculated, following the procedure described in [10].

Since in p–A both Drell–Yan [16, 13] and open charm production [17] are experimentally known to scale as  $A^\alpha$ , with  $\alpha_{DY} = \alpha_{D\bar{D}} = 1$ , the four mass spectra have been fitted simultaneously, imposing  $\sigma_{D\bar{D}}/\sigma_{DY}$  to be constant. Fits have been performed either fixing the contribution of the combinatorial backgrounds with the procedure described in the previous section, or leaving their absolute normalizations free, to eventually improve the description of the measured mass shape. Both fits satisfactorily describe the mass spectra; the free background option gives, as expected, a slightly better  $\chi^2/ndf$ . Figure 2 shows the invariant mass spectrum measured in p–W collisions, together with the result of the fit; the superposition of the expected sources gives a good description of the dimuon yield.

The normalization of the  $D\bar{D}$  contribution to the mass spectra varies by  $\sim 20\%$  between the two fitting procedures; this provides an evaluation of the systematic error connected with the combinatorial background subtraction.

The S–U and Pb–Pb spectra have been fitted with the same procedure adopted for the p–A data samples, without any constraint on the  $\sigma_{D\bar{D}}/\sigma_{DY}$  ratio. The normaliza-

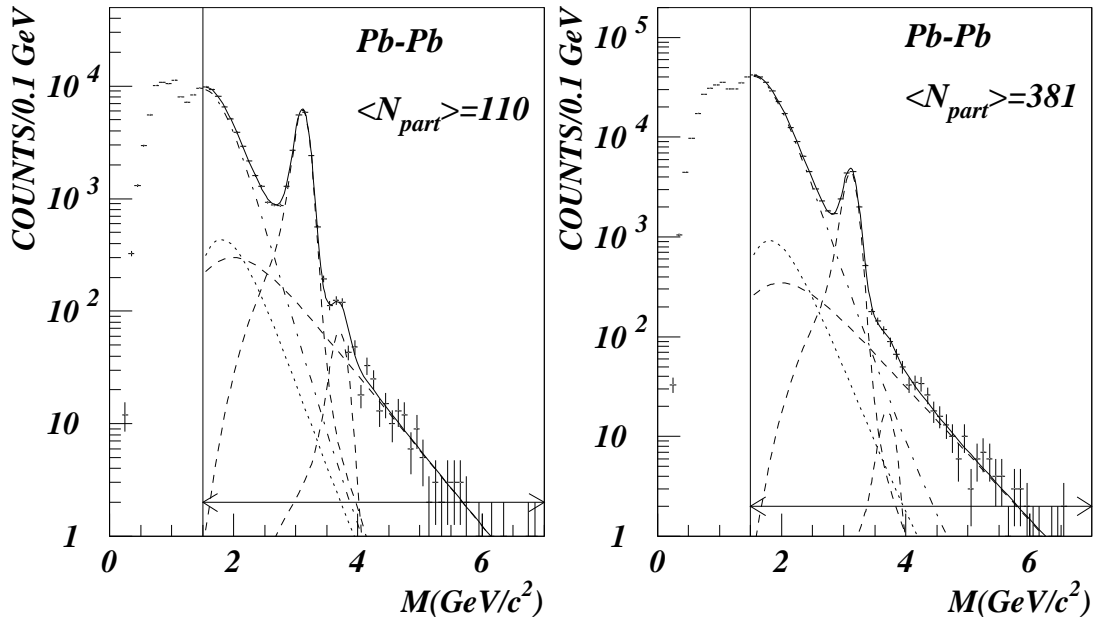


Figure 3: Fit to peripheral and central Pb–Pb spectra. The  $DY$ ,  $J/\psi$  and  $\psi'$  contributions are shown as dashed lines, the open charm as a dotted line, the background as a dashed–dotted line.

tion of the combinatorial background was again fixed with the procedure described in section 3. As a result, the 9 Pb–Pb, and the 5 S–U mass spectra have been satisfactorily described by a superposition of the four dimuon sources used in the fit; however, for both systems, the number of  $D\bar{D}$  dimuons is found to increase with the centrality of the collision, with respect to  $DY$ . This is illustrated in fig. 3, where the fits to a peripheral and a central Pb–Pb mass spectrum can be compared.

Since, as already pointed out, the Drell–Yan process is known to scale as  $A \cdot B$  in A–B collisions, and the open charm is expected to have the same behaviour, the observed feature indicates that dimuons from open charm decays are abnormally enhanced in nucleus–nucleus collisions. Quantitatively speaking, the open charm contribution fitted from the IMR is enhanced by a factor  $\sim 1.5$  in central S–U collisions with respect to peripheral; the corresponding factor in Pb–Pb is  $\sim 2$ .

#### 4.4 Size of the enhancement

We have already shown that in p–A collisions the IMR can be described as a superposition of dimuons due to Drell–Yan, determined unambiguously by a fit to the HMR, plus a component which has the mass shape of dimuons from open charm.

That component is abnormally enhanced in central nucleus–nucleus collisions.

We will now compare the open charm yield, as inferred by its dimuon decay, both between the various systems (p–A, S–U, Pb–Pb), and with direct measurements of charm hadron production. In a recent paper [18], results of various CERN and FNAL open charm hadro–production experiments have been reviewed. The  $\sqrt{s}$  dependence of  $D$  meson cross sections, within a factor  $\sim 2$  which can be attributed to residual systematical errors, has been found to be well described by PYTHIA; the differential distributions of the  $D$  mesons, as well as the lepton distributions from their semi–leptonic decays measured in several experiments, have been checked to be in good agreement with PYTHIA calculations. To match the experimental points, the absolute normalization provided by PYTHIA must be scaled up by an appropriate  $K$ -factor.

Since PYTHIA has been verified to reproduce the dilepton spectra from open charm, it should be possible, starting from the yield of open charm decays estimated in this analysis, whose mass shape has also been calculated with PYTHIA, to derive indirectly an absolute open charm cross section. Such a calculation has been carried out for the p–A data; in fig. 4 the per–nucleon cross section for forward  $c\bar{c}$  production, extrapolated from the analysis of the p–A data previously described, is compared with results of direct open charm measurements.

The dotted line shows the  $\sqrt{s}$  dependence predicted by PYTHIA, upscaled by a  $K$ -factor, satisfactorily reproducing most of the experimental points. The NA50 value extracted from this analysis is found to be compatible with the others.

Similarly, the S–U and Pb–Pb per nucleon open charm cross sections can be extrapolated from the results of the fits to the mass spectra and compared, at the relevant energies, with the points in fig. 4. As a reference, either the dotted line of fig. 4, or the same line, re–scaled to match the NA50 p–A result, can be taken. The enhancement  $E$  of the charm component with respect to the second reference, i.e. to the  $c\bar{c}$  cross section normalized to the NA50 p–A point, is shown in fig. 5, versus the number of participant nucleons  $N_{part}$ . The enhancement clearly increases with  $N_{part}$ ; in central Pb–Pb collisions the dimuon yield from open charm decays is 3 times higher than expected from a linear extrapolation of the observed p–A yield.

## 4.5 The $p_T$ spectra of IMR dimuons

Since no reconstruction of the  $D$ -meson decay can be performed with the NA38/NA50 experimental apparatus, any unknown contribution which might happen to give, in the acceptance of the experiment, a mass shape similar to the one induced by charmed meson decays, could be an alternative origin of the excess observed. It is therefore important to check if the distributions of other kinematical variables of IMR dimuons are well described by a superposition of the various known sources, having fixed their relative weights to the values found in the fit of the invariant mass spectra. Figure 6 shows the  $p_T$  distributions of dimuons in the mass region  $1.5 < M_{\mu\mu} < 2.5$  GeV/ $c^2$  measured in peripheral and central Pb–Pb collisions. The normalizations of the  $DY$

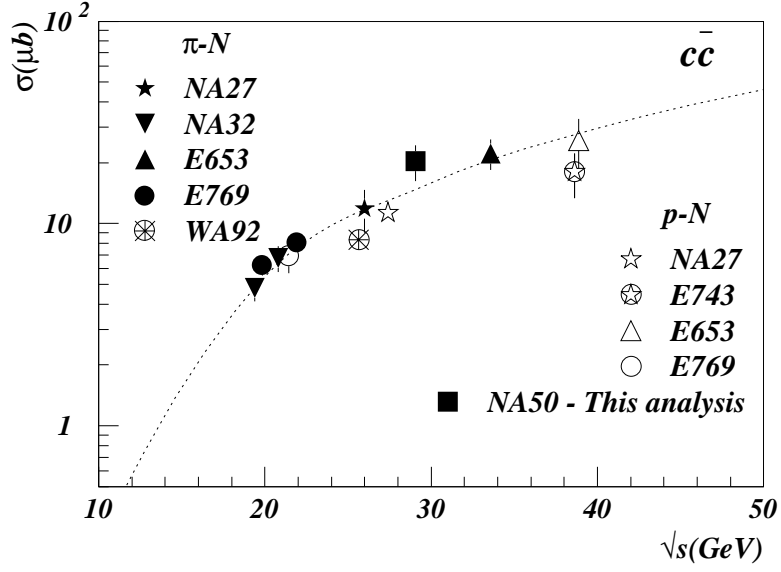


Figure 4: Cross sections for forward ( $x_F > 0$ )  $c\bar{c}$  production compared with the value extrapolated from this analysis.

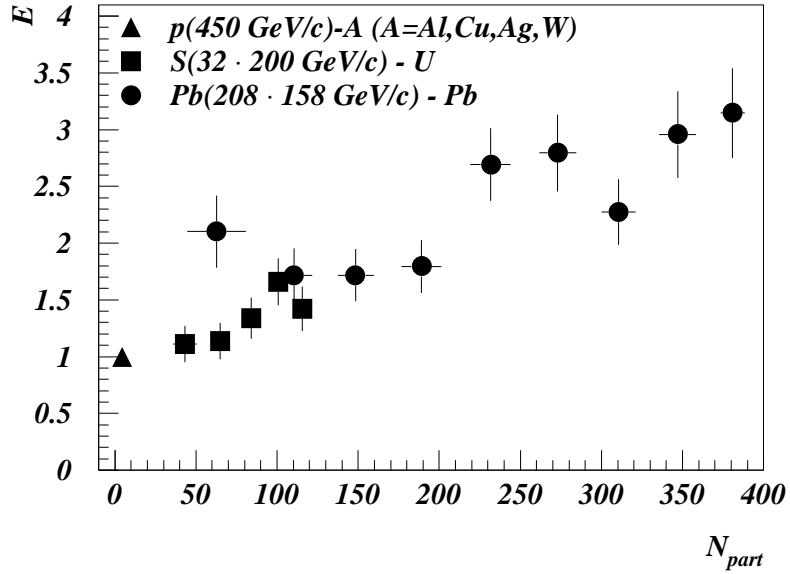


Figure 5: The enhancement factor  $E$  of the open charm dimuon component with respect to p-A collisions vs the number of participant nucleons  $N_{part}$ .

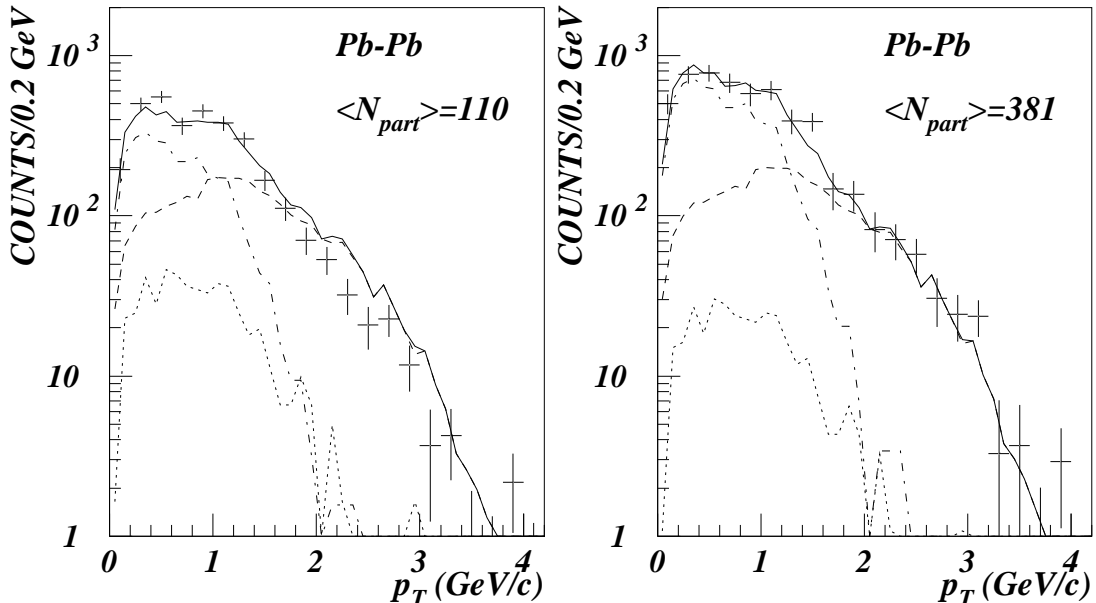


Figure 6: The  $p_T$  distribution of IMR dimuons for peripheral and central Pb–Pb collisions. The  $DY$  (dashed line),  $J/\psi$  (dotted line) and  $D\bar{D}$  (dashed-dotted line) contributions, as well as their sum (solid line) is also shown.

and  $D\bar{D}$  contributions are taken from the mass analysis, i.e. including the charm enhancement reported in figure 5. The low mass tail of the  $J/\psi$  is also taken into account. The agreement between the data and the sum of the various sources is very good, supporting the hypothesis that the excess dimuons come from open charm decays.

## 5 Conclusions

The intermediate mass muon pair continuum measured by the NA50 experiment in p–A collisions can be described in terms of the well known sources:  $DY$  and  $D\bar{D}$ . In S–U and Pb–Pb interactions a satisfactory description of the mass spectra can also be obtained, provided we assume that the dimuon production from open charm is enhanced with respect to the QCD expectations. The enhancement factor seems to increase linearly with the number of participants. In central Pb–Pb collisions a factor 3 enhancement is necessary to describe the data. The analysis of the IMR  $p_T$  spectra provides further support to the hypothesis that the excess dimuons come from open charm decays.

## References

- [1] see e.g. Ruuskanen P.V., *Nucl.Phys.***A544**(1992)169c for an overview on the subject
- [2] Lourenço C. et al. (NA38 collaboration), *Nucl.Phys.* **A566**(1994)77c
- [3] Scomparin E. et al. (NA50 collaboration), *Nucl.Phys.* **A610**(1996)331c
- [4] Angelis A.L.S. et al. (HELIOS/3 collaboration), preprint CERN-EP/98-92
- [5] Anderson L. et al., *Nucl.Inst.Meth.***223**(1984)26
- [6] Baglin C. et al. (NA38 collaboration), *Phys.Lett.* **B220**(1989)471
- [7] Abreu M.C. et al. (NA50 collaboration), *Phys.Lett.* **B410**(1997)327
- [8] Bellaiche F. et al., *Nucl.Inst.Meth.***A398**(1997)180
- [9] Arnaldi R. et al., *Nucl.Inst.Meth.***A411**(1998)1
- [10] Fleuret F., Thesis, Ecole Polytechnique, Palaiseau (1997)
- [11] Werner K., *Phys. Rep.***232**(1993)87
- [12] Constantinescu S. et al., preprint IPNO-DRE-96-01
- [13] Abreu M.C. et al. (NA50 collaboration), *Phys.Lett.* **B410**(1997)337
- [14] Sjostrand T., *Computer Physics Commun.***82**(1994)74
- [15] Martin A.D. et al., *Phys.Rev.***D51**(1995)4756
- [16] Alde D.M. et al. (E772 collaboration), *Phys.Rev.Lett***64**(1990)2479
- [17] Leitch M.J. et al. (E789 collaboration), *Phys.Rev.Lett***72**(1994)2542
- [18] Braun-Munzinger P. et al., *Eur.Phys.J.***C1**(1998)123